AD-A105 172 TRITEC INC COLUMBIA MD F/G 9/5
ADVANCED ELECTROFLUIDIC SERVOVALVE DEVELOPMENT.(U)
AUG 81 L K PECAN DAAK51-80-C-0017
UNCLASSIFIED USAAVRADCOM-TR-81-D-30 NL

1 OF 1
ADA
105172

END
DATE
FILMED
10-81
DTIC

USAAVRADCOM-TR-81-D-30

LEVEL II

12

AD A105172

ADVANCED ELECTROFLUIDIC SERVOVALVE DEVELOPMENT

Lester K. Pecan
TRITEC, INC.
P.O. Box 56
Columbia, Maryland 21045

August 1981

Final Report for Period April 1980 - April 1981

Approved for public release;
distribution unlimited.

Prepared for

APPLIED TECHNOLOGY LABORATORY
U. S. ARMY RESEARCH AND TECHNOLOGY LABORATORIES (AVRADCOM)
Fort Eustis, Va. 23604

APPLIED TECHNOLOGY LABORATORY POSITION STATEMENT

This report has been reviewed by the Applied Technology Laboratory, U.S. Army Research and Technology Laboratories (AVRADCOM), and is considered to be technically sound.

This research effort resulted from the need which exists for a dual input (electrical and fluidic) servovalve for military vehicles. The potential exists for eventually equipping these vehicles with electrical or fluidic controlling systems as well as combinations of these systems. An electro-fluidic servovalve would provide the U.S. Army with the capability of transforming electrical and fluidic control input signals into mechanical motion of a single servoactuator rather than two separate servoactuators, thereby reducing cost, weight, and complexity.

This program investigated the use of the rotating movable flow splitter fluid amplifier, an actuator piston feedback mechanism, and a positive derivative feedback circuit. The positive derivative feedback circuit controls spool response, so that flow to the actuator is proportional to actuator velocity.

Mr. George W. Fosdick of the Applied Aeronautics Technical Area, Aeronautical Systems Division, served as project engineer for this effort.

UNCLASSIFIED

SECURITY CLASSIFICATION OF THIS PAGE (When Data Entered)

REPORT DOCUMENTATION PAGE		READ INSTRUCTIONS BEFORE COMPLETING FORM
1. REPORT NUMBER (18) (19) USAAVRADCOM-TR-81-D-30	2. GOVT ACCESSION NO. AD-A105 171	3. RECIPIENT'S CATALOG NUMBER
4. TITLE (and Subtitle) (6) ADVANCED ELECTROFLUIDIC SERVOVALVE DEVELOPMENT.		5. TYPE OF REPORT & PERIOD COVERED (9) Final Report, April 1980 - April 1981,
		6. PERFORMING ORG. REPORT NUMBER
7. AUTHOR(s) (10) Lester K. Pecan		8. CONTRACT OR GRANT NUMBER(s) (15) DAAK51-80-C-0017
9. PERFORMING ORGANIZATION NAME AND ADDRESS TRITEC, INC. P.O. Box 56 Columbia, Maryland 21045 (17) 00		10. PROGRAM ELEMENT, PROJECT, TASK AREA & WORK UNIT NUMBERS (16) 62209A 1L162209AH25 00 320 EK
11. CONTROLLING OFFICE NAME AND ADDRESS Applied Technology Laboratory, U.S. Army Research & Technology Laboratories (AVRADCOM) Fort Eustis, Virginia 23604 (11)		12. REPORT DATE August 1981
		13. NUMBER OF PAGES 46 (12) 47
14. MONITORING AGENCY NAME & ADDRESS(if different from Controlling Office)		15. SECURITY CLASS. (of this report) UNCLASSIFIED
		15a. DECLASSIFICATION/DOWNGRADING SCHEDULE

16. DISTRIBUTION STATEMENT (of this Report)

Approved for public release; distribution unlimited.

17. DISTRIBUTION STATEMENT (of the abstract entered in Block 20, if different from Report)

18. SUPPLEMENTARY NOTES

19. KEY WORDS (Continue on reverse side if necessary and identify by block number)

Electrofluidic Servovalves	Hydrofluidics
Fluerics	Servoactuators
Fluidics	Servovalves
Flight Control Systems	Stability Augmentation

20. ABSTRACT (Continue on reverse side if necessary and identify by block number)

This report covers the advanced development of an electrofluidic servovalve. This device accepts and sums electrical and hydraulic inputs and provides an output capable of accurately positioning a hydraulic actuator. The design employs fluidic amplifiers with rotating movable flow splitters, an actuator piston feedback mechanism, and a unique positive derivative feedback circuit. The need for adequate actuator flow is met by use of a spool valve to augment the driving amplifier output. The positive

1
F

DD FORM 1 JAN 73 1473 EDITION OF 1 NOV 65 IS OBSOLETE

UNCLASSIFIED 393775

SECURITY CLASSIFICATION OF THIS PAGE (When Data Entered) derivative feedback circuit controls spool response, so that flow to the actuator is proportional to actuator velocity. Demonstration tests of the final design showed satisfactory performance of the rotary splitter concept, and an order-of-magnitude increase in servovalve frequency response through use of derivative feedback.

Accession For	
NTIS GRA&I	X
DTIC TAB	☐
Unannounced	☐
Justification	
By	
Distribution/	
Availability Codes	
Dist	Avail and/or Special
A	

1
B

SUMMARY

This report covers the advanced development of an electrofluidic servovalve. This device accepts and sums electrical and hydraulic input signals and provides an output capable of accurately positioning a hydraulic actuator. The design employs two stages of fluidic amplifiers, an actuator position feedback mechanism, and a unique positive derivative feedback circuit. Electrical signals are converted by an electrical motor to displacement of a movable jet flow splitter in the first stage amplifier. Actuator position is fed back to the second stage amplifier movable jet flow splitter. The need for adequate flow to the actuator is met by use of a spool valve to augment the driving amplifier flow. The positive derivative feedback circuit controls spool response so that flow to the actuator is proportional to actuator piston velocity, thereby greatly enhancing the servovalve frequency response and damping characteristics.

In an earlier program a breadboard model of the servovalve was used to demonstrate the feasibility of the movable splitter and derivative feedback concepts. However, the results of the earlier program showed the need for further study and redesign to improve amplifier gain, reduce movable splitter vibration and friction, and to improve the derivative feedback performance and reliability. In this program, a mathematical model of the servovalve was used to define the optimum values of all critical parameters. In addition, tests were conducted to establish all significant pressures, velocities, and phase relationships. From this, an operational envelope was established. Components were sized to be compatible with this envelope, and performance demonstrations were conducted. In the course of testing, variations of the movable splitter concept were evaluated, and a rotational splitter was developed to replace the original translating design. Performance tests showed the following achievements:

- Reduced rotary splitter friction compared to the translating splitter.
- Freedom from splitter vibration and structural fatigue.
- Linear amplifier output proportional to rotary splitter angular position.
- Mathematical model validity confirmed.
- Ability of rotary splitter to sum fluidic and displacement inputs.
- A twofold increase in amplifier pressure gain through use of rotary splitter.

- Order-of-magnitude increase in servovalve bandwidth through use of derivative feedback.

Modification of the amplifiers to incorporate rotational splitters invalidated the earlier use of a torque motor to accept electrical input signals. Torque motors typically have an operational range of less than 1°, whereas the rotary splitter operates over a ±25° range. Although a mechanical linkage could be designed to couple a torque motor to the rotational splitter, it is recommended that alternate means of accommodating electrical inputs be investigated before a final decision is made.

As a result of this program, sufficient data and experience are now available to permit advancement to the next recommended step: design, fabrication, and test of a pre-production prototype.

PREFACE

This document is the final report on the advanced development of an electrofluidic servovalve. The work was performed by TRITEC, INC. of Columbia, Maryland during the period April 1980 through April 1981 under Contract DAAK51-80-C-0017. The Applied Technology Laboratory, U.S. Army Research and Technology Laboratories (AVRADCOM), Fort Eustis, Virginia, sponsored the program, with Mr. George Fosdick as the Contracting Officer's Technical Representative.

TABLE OF CONTENTS

LIST OF ILLUSTRATIONS

INTRODUCTION

In an earlier program (Reference 1), TRITEC, INC. designed, fabricated, and tested a breadboard model of a dual input electrofluidic servovalve (Figure 1). This device accepts electrical and hydraulic input signals and provides a hydraulic output capable of driving a hydraulic actuator. The model employs fluidic amplifiers, an actuator position feedback mechanism, and a unique positive derivative feedback circuit. Electrical signals are converted by means of a torque motor into translation of a movable flow splitter in the first stage amplifier. A second stage amplifier drives the actuator. Actuator position is fed back to a movable splitter in the second stage amplifier. The need for adequate flow to the actuator is met by use of a spool valve to augment the driving amplifier flow. The positive derivative feedback circuit is used to control spool response so that flow to the actuator is in proportion to actuator velocity.

Test and evaluation of the servovalve demonstrated feasibility of the concept. However, the tests revealed several areas where further study and redesign were required. These areas included:

- Movable splitter redesign to improve amplifier gain and reduce splitter vibration.
- Positive derivative feedback circuit redesign to improve performance.
- Position feedback mechanism redesign to reduce the mechanical complexity and size of the linkage.

The present program had as its objective the redesign of the breadboard components to eliminate the shortcomings revealed by the original tests. A unique and significant feature of the servovalve is the positive derivative feedback circuit. Proper functioning of this circuit permits control of system damping and increase in bandwidth without the penalty of increased amplifier leakage flow, which would be incurred if larger amplifiers were used. Tests of the original breadboard showed that the servovalve performance was improved by use of the positive derivative feedback, but the improvement was marginal and performance was erratic. In the current

---

1 M. F. Funke, and L. K. Pecan, THE DESIGN, FABRICATION, AND TEST OF AN ELECTROFLUIDIC SERVOVALVE, TRITEC, INC.; Applied Technology Laboratory, U.S. Army Research and Technology Laboratories (AVRADCOM), Fort Eustis, Virginia, February 1980, AD A082443.

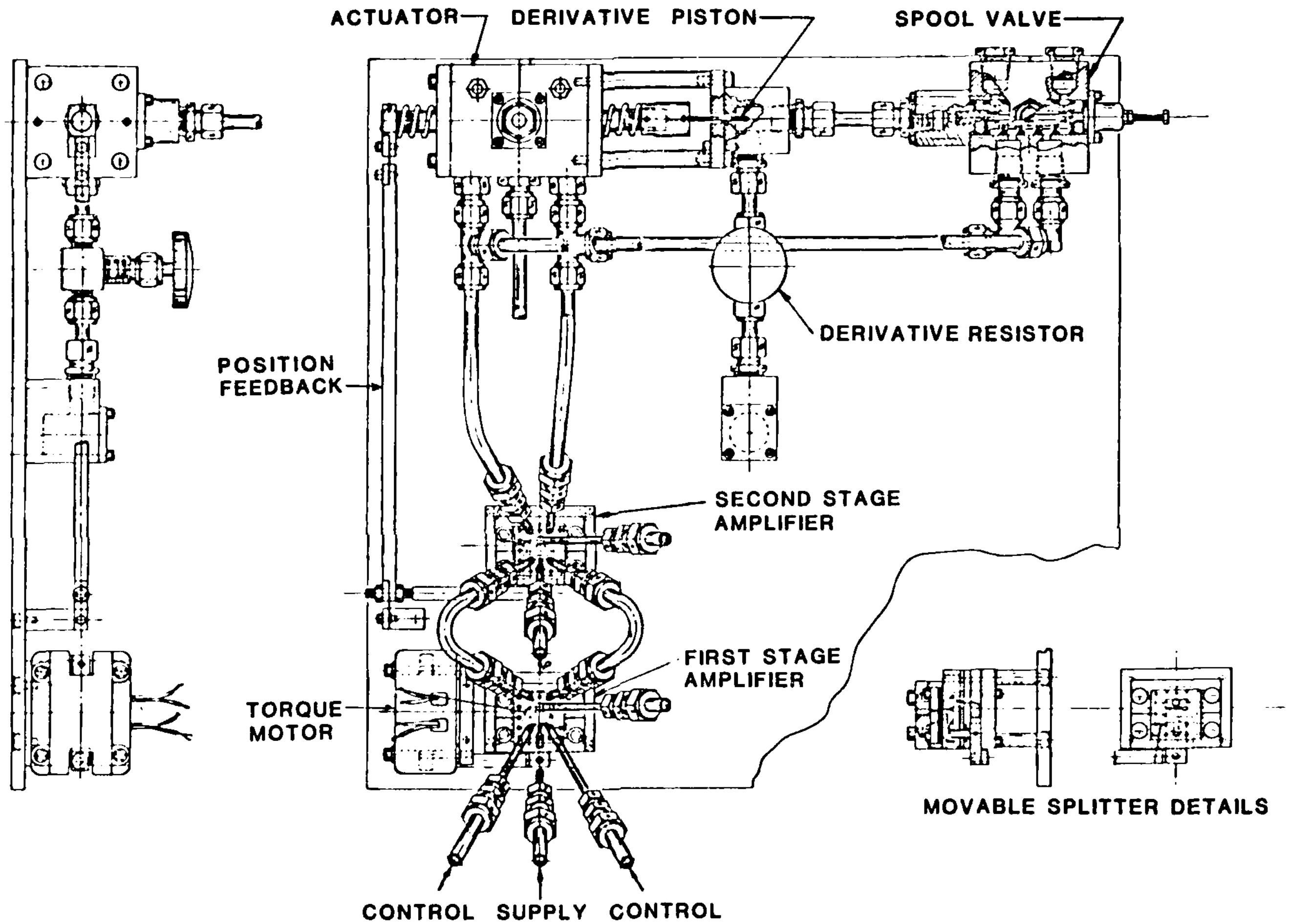

Figure 1. Servovalve breadboard arrangement.

effort, the performance data of the derivative feedback circuit was analyzed, new test data was obtained, critical components of the circuit were resized, and proper performance was demonstrated by retest.

The ability to accept and implement input signals and to control actuator position by means of a movable flow splitter is also a key feature of the servovalve design. In the earlier program, a translating splitter was used. However, the physical shape and mechanization of the splitter resulted in low amplifier gain, splitter vibration, high friction, and hysteresis. In the present program, alternate splitter shapes and motion mechanisms were evaluated. As a result, a rotating, tapered splitter was developed. This concept was shown to overcome most of the shortcomings of the earlier device, with a significant improvement in amplifier gain and output linearity.

Although the current program concentrated on redesign and test at the component level, overall servovalve performance was also demonstrated by system-level tests of the reassembled breadboard.

SERVOVALVE DESCRIPTION

The main components of the servovalve are:

- First stage amplifier which accepts and sums input signals; drives second stage amplifier.
- Second stage amplifier which drives the actuator and responds to actuator position feedback signals.
- Position feedback link which transmits actuator position to second stage amplifier movable splitter.
- Positive derivative feedback circuit which provides flow to the actuator in response to actuator velocity.

Figure 2 is a block diagram showing the components and their relationship to the actuator. Figure 3 is a simplified diagram of the internal design of the components. To illustrate the operation of the servovalve, assume that the mechanical input link of Figure 3 is moved to the right. This motion causes clockwise rotation of the splitter in the first stage amplifier, diverting the amplifier jet toward the right hand receiver. The output of the first stage amplifier, driving the second stage amplifier, causes the second stage output jet to be moved to the left.

The second stage output now supplies a higher pressure to the left-hand side of the actuator piston, causing it to move to the right. As the piston moves to the right, the position feedback link causes the second stage splitter to rotate in a clockwise direction. This splitter rotation has an opposing influence on the amplifier jet, nulling the output when the desired actuator position is reached. The same motion of the actuator could have been accomplished by applying an input pressure differential to the first stage amplifier. A combination of electrical (or mechanical) and pressure inputs could also be applied, with the resulting actuator motion being the sum total of those that would have resulted from the electrical and pressure signals being applied separately. Thus, the first stage amplifier also acts as a summing device.

The speed of response of the actuator is limited by the output flow from the driving amplifier. If a small amplifier is used to reduce leakage flow within the amplifier, the speed of response is low. To overcome this speed of response problem, large driving amplifiers have previously been used, and large leakage flow penalties have been incurred.

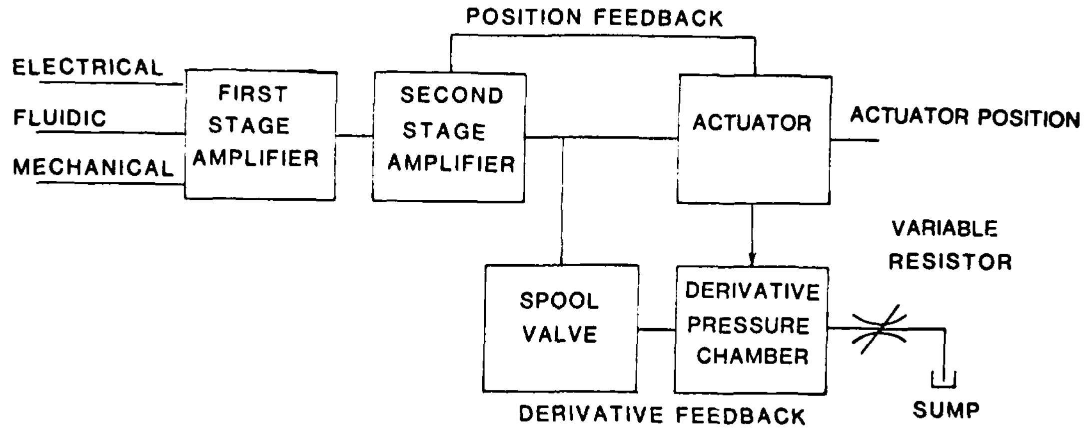

Figure 2. Servovalve component block diagram.

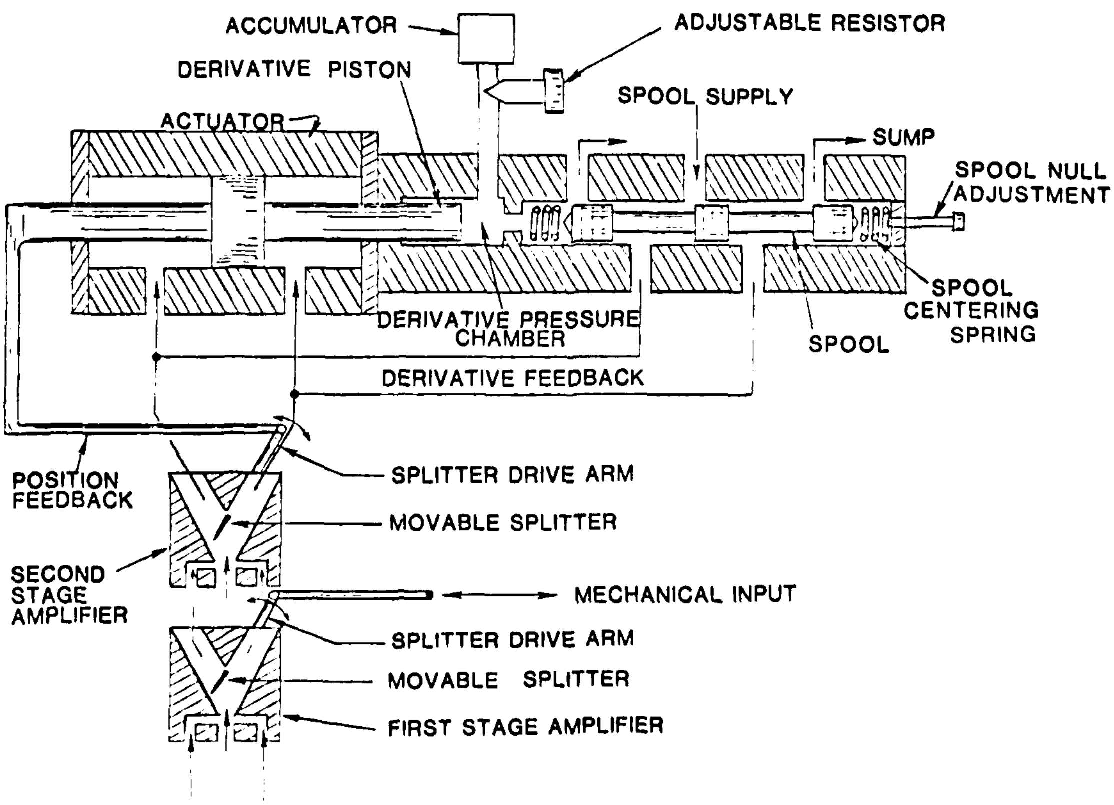

Figure 3. Schematic of servovalve.

Both increased speed of response and lower leakage are simultaneously achieved by the use of positive derivative feedback. Referring again to Figure 3, note that motion of the actuator causes a corresponding motion of the derivative piston, in this case to the right. With the resistor valve closed, this causes a rapid pressure rise in the piston cavity, resulting in a relative motion of the spring-centered spool to the right. Adjustment of the resistor valve regulates the magnitude of pressure rise in the piston cavity and consequently the amplitude of spool motion. As will be shown later, the pressure rise (or decrease if the derivative piston motion is to the left) is proportional to the velocity of the piston and is therefore derivative in nature and thus reduces system damping. With the spool valve flow augmenting the amplifier output flow to the actuator piston, a highly responsive actuator motion is achieved. Note that when the piston reaches its commanded position, motion ceases. With no velocity to sustain a pressure differential in the derivative piston chamber, the spool returns to its centered position, shutting off flow to the actuator. It should be emphasized that the flow from the spool valve is not dependent on the ΔP signal across the actuator, but only on the rate of actuator piston travel. Adjustment of the resistor valve controls the speed of response of the actuator.

The present servovalve uses a rotating, wedge-shaped flow splitter. In the course of developing this configuration, other variations were tested. As shown in Figure 4, the splitter motion could be translatory and the shape could be parallel-sided.

Of the three alternates, the rotating design resulted in the lowest friction and best performance. Earlier versions were made from flattened, 0.025-in.-diameter steel wire mounted in either a cubic block (translating) or a cylindrical platform (rotating). However, this arrangement was not structurally adequate. Splitter vibration caused noisy output and eventual fatigue failure of the splitter. As a result, a means was devised to machine the splitter integrally with the rotating drive rod as shown in Figure 5. This design has performed well, with no structural problems developing throughout the program.

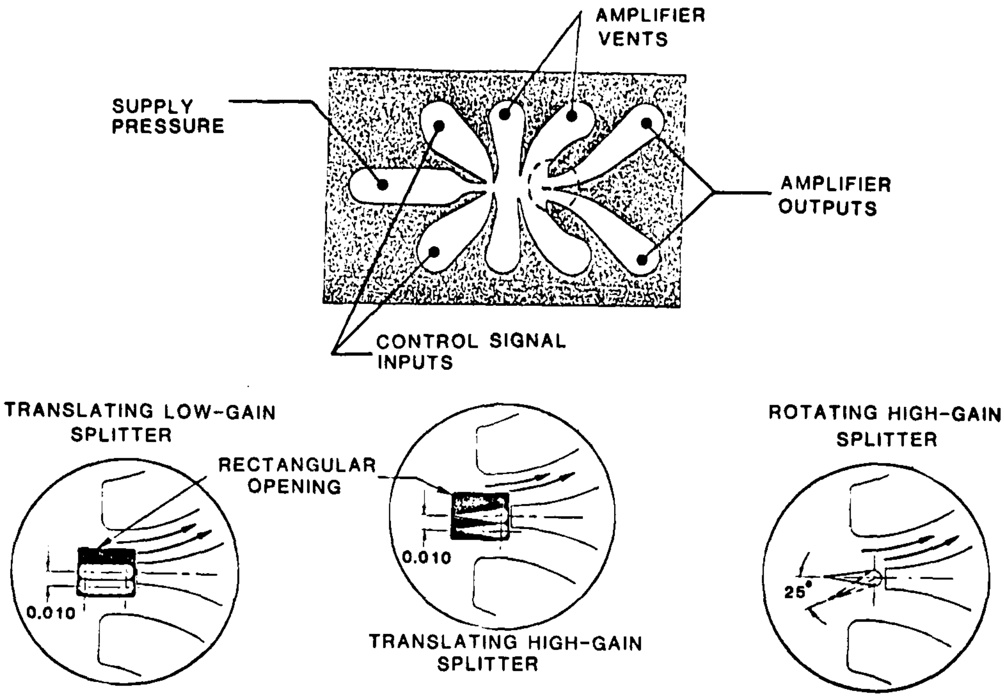

Figure 4. Movable splitter concepts.

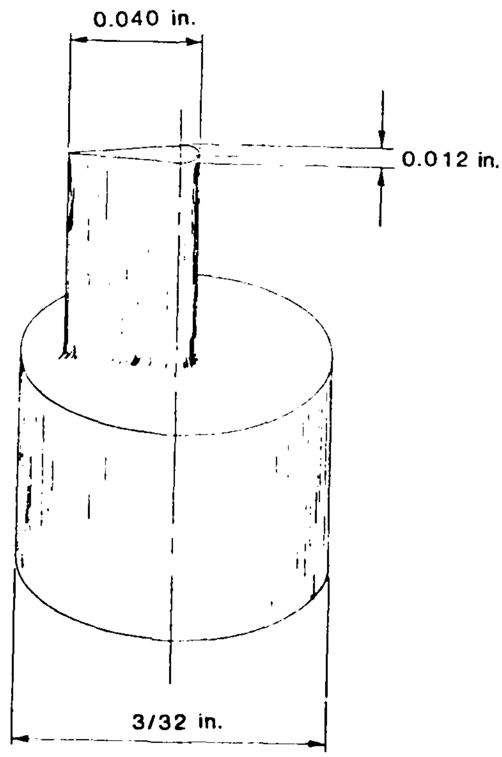

Figure 5. Enlarged view of rotary splitter.

PERFORMANCE PREDICTIONS

In order to establish performance requirements for the servovalve components, it is first necessary to define system-level performance parameters. With system-level performance established, the required component contributions can be examined and performance specifications set. To accomplish this, it is advantageous to set up a mathematical model of the servovalve. Then, by using established techniques, the dynamic response characteristics of the servovalve can be predicted.

Figure 6 is a block diagram representing the servovalve shown in Figures 1 and 2.

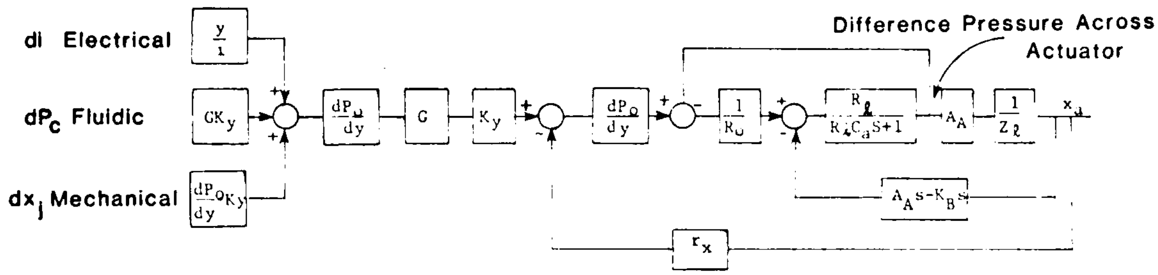

Figure 6. Servovalve block diagram.

Figure 6 symbols:

$\frac{y}{i}$ = Torque motor displacement coefficient, in./amp

G = Pressure gain

K_y = Jet displacement at splitter for pressure input, in./psi

$\frac{dP_o}{dy}$ = Output difference pressure (blocked output) for jet displacement at splitter, psi/in.

R_o = Driving amplifier output resistance, lb sec/in.^{5}

R_ℓ = Leakage resistance across actuator, lb sec/in.^{5}

C_a = Actuator compliance, in.^{3}/psi

A_A = Actuator piston area, in.^{2}

Z_ℓ = Load impedance, lb/in.

r_x = Position feedback ratio

K_B = Derivative feedback, in.^{2}

s = Laplace operator, sec.$^{-1}$

The input (di, dP_C, dx_j) to the valve gives rise to a jet deflection (y). Through the amplifier characteristic, dP_o/dy, a pressure differential exists across the splitter. This pressure across the splitter generates a flow into one side of the actuator cylinder. By virtue of the change of volume, flow is integrated. In addition, a differential pressure is generated across the actuator piston. This differential actuator pressure feeds back to the input summing junction to reduce the ΔP across the driving amplifier output resistor. This differential pressure also acts on the actuator piston area, A_A, to develop a net force differential across the actuator piston. This force, divided by the load impedance Z_ℓ, defines the actuator displacement x_a. The actuator piston displacement feeds back on the actuator flow summing junction in two ways: by means of the swept volume and the derivative feedback.

The feedback block A_As-K_Bs is a significant feature. The A_As term is the swept volume flow and represents a system damping element common to all servovalves. For small fluidic elements it results in severe overdamping. The A_As term gives rise to a time constant which must simply be accepted as a valve response limiting factor. However, the K_Bs term of the positive derivative control provides a means of offsetting this inherent servovalve limitation. It also provides a means of eliminating the lag of the swept volume of the actuator piston motion. Thus, not only can damping be tailored to achieve optimum system performance, but system speed-of-response can be increased beyond that attainable by the fluidic amplifier alone.

Closing the loop between the piston position x_a and the input jet deflection is the feedback element r_x. The value of r_x can be adjusted mechanically to obtain any desired displacement for a given input command. Note that actuator piston displacement is fed directly back to the driving amplifier movable splitter; thus it is unaffected by changes in viscosity due to temperature variations.

The inner loop of Figure 6 can be reduced to the form shown in Figure 7.

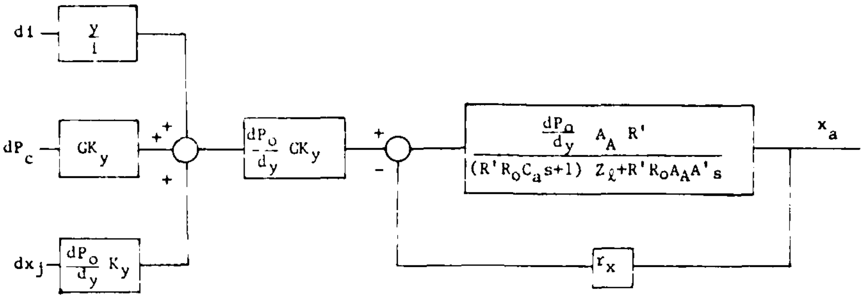

Figure 7. Servovalve block diagram reduction.

In Figure 7 the feedback element $A_A - K_B$ has been replaced by the symbol A' for convenience. Inclusion of a general quadratic form for the load Z_ℓ in the characteristic function of the reduced inner loop yields:

$$(R'R_oC_a s + 1)\ (Ms^2 + Bs + K)\ +\ R'R_o\ A_A\ A's \qquad (1)$$

where

M is the load mass, lb sec^2/in.

B is load viscous damping, lb sec/in.

K is load spring rate, lb/in.

The system bandwidth may be found by setting the characteristic expression (1) equal to zero and finding the roots of the resulting equation. In general, the solution will yield one real root and a complex conjugate pair of roots. Factoring the equation using these roots permits determination of the simple lag frequency and the quadratic, or second order, frequency. The effects of derivative feedback can be determined by solving expression (1) for a range of values of the feedback parameter A'. For convenience, the feedback ratio A'/A_A can be used as a measure of derivative feedback. With no derivative feedback ($K_B = 0$), $A' = A_A$ and the ratio A'/A_A equals unity. As the extent of derivative feedback increases, A'/A_A becomes smaller. When the value of K_B exceeds that of A_A, A' becomes negative and the system becomes unstable. The system performance predictions, therefore, are made for a range of A'/A_A approaching zero but not becoming negative.

By varying A'/A_A from 0.001 to 1.0 and using the following system parameter values, the curves of Figure 8 are obtained.

R_O = 250 psi/cis (obtained by measurement)

R = $10R_O$ (estimate based on test measurements)

C_a = 4.6×10^{-6} in.^{3}/psi (calculated)

A_A = 0.20 in.^{2} (actuator design value)

M = 0.001 lb sec^2/in. (measured)

K = 20 lb/in. (measured)

B = 0.2828 lb sec/in. (estimated load damping of 1.0)

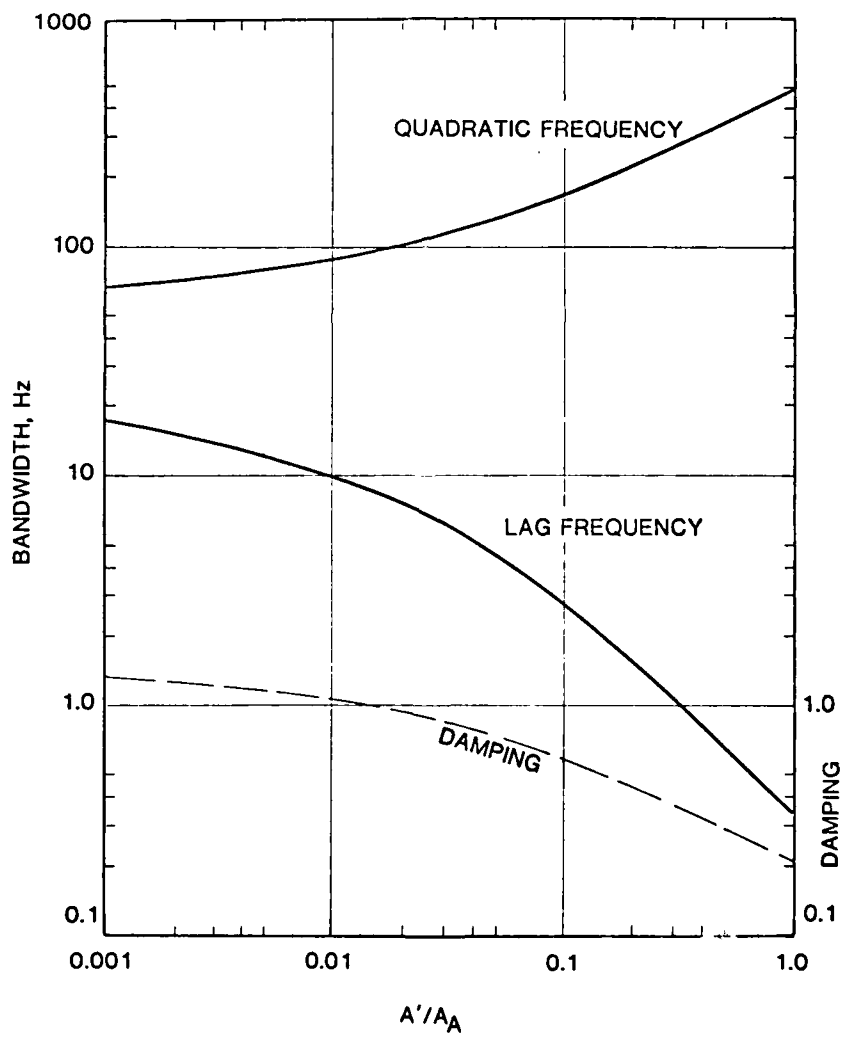

Figure 8. Predicted system performance.

Examination of Figure 8 shows that the system performance is dominated by the first order response, since the quadratic contribution is of the order of 100 Hz, or greater, beyond our range of interest. The curves show that the servovalve without derivative feedback has a calculated bandwidth of between 0.3 and 0.4 Hz (the actual value, as measured during the earlier program of Reference 1 was 0.45 Hz). The curves also show a predicted increase in bandwidth to almost 3.0 Hz for a value of $A'/A_A = 0.1$, an increase of almost one order of magnitude. In order to achieve this performance, it is necessary that the component performance levels meet those assumed for the calculations. To assure this, we first examine in detail the component requirements of the derivative feedback elements.

DERIVATIVE FEEDBACK PERFORMANCE

To understand how the derivative feedback requirements can be implemented, it is necessary to examine the feedback element K_B in detail. The block diagram of Figure 9 relates the actuator stroke x_a to the spool flow.

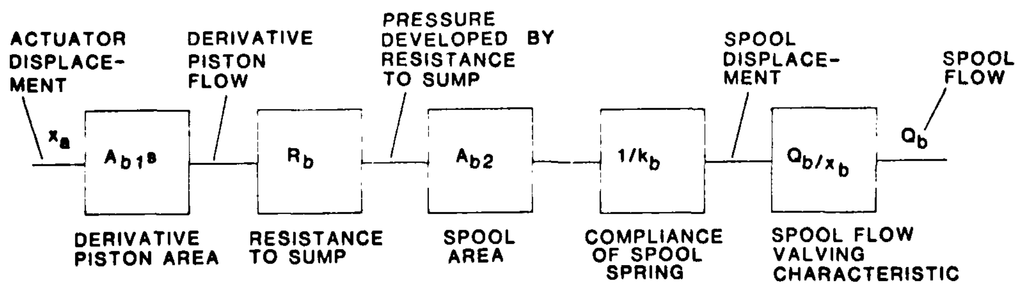

Figure 9. Block diagram of derivative feedback term.

The diagram in Figure 9 reduces to:

$$Q_b/x_a = \frac{A_{b1}}{k_b} \frac{A_{b2} R_b Q_b}{x_b} s = K_B s \tag{2}$$

Equation (2) permits us to size the elements of the derivative feedback circuit. The spool flow characteristic Q_b/x_b can be measured by advancing the spool with a micrometer screw drive and measuring the resulting flow. However, when the spool valve is operated by derivative piston pressure, there is no convenient way to monitor spool motion, since the free spool is inaccessible within the spool valve housing. Therefore, a criterion is necessary to demonstrate spool response, and consequently flow response, to derivative piston pressure. Equation (2) can be rewritten:

$$Q_b = (x_a A_{b1} R_b) s \frac{A_{b2}}{k_b} \frac{Q_b}{x_b} \tag{3}$$

In equation (3) it is seen that the quantity $(x_a A_{b1} R_b)s$ is the pressure developed by the derivative piston. Letting $(x_a A_{b1} R_b)s = P_b$ and substituting this into equation (3) we obtain:

$$\frac{Q_b}{P_b} = \frac{A_{b2}}{k_b} \times \frac{Q_b}{x_b} \tag{4}$$

Since Q_b/P_b can be measured, it can be used as a criterion to test the spool valve-derivative piston assembly. Measurements made on the spool valve (Figure 10) show that with a 100 psi supply pressure, the spool flow characteristic Q_b/x_b = 80 cis/in. Substituting this value and the known values for the spool area and spool spring rate into equation (4) we obtain:

$$\frac{Q_b}{P_b} = \frac{(0.0308)(80)}{50} = 4.93\ (10^{-2})\ \text{cis/psi} \tag{5}$$

Equations (3) and (4) are based on the assumption that the pressure P_b is a function of the actuator and derivative piston velocity, and that as a result of the development of P_b, the spool will indeed move and provide the required flow, Q_b. To demonstrate the validity of this, the derivative feedback circuit can be tested by harmonic oscillation of the derivative piston at controlled frequencies and amplitudes. Under these conditions the time history of input displacement and velocity are known, and the resulting time history of P_b

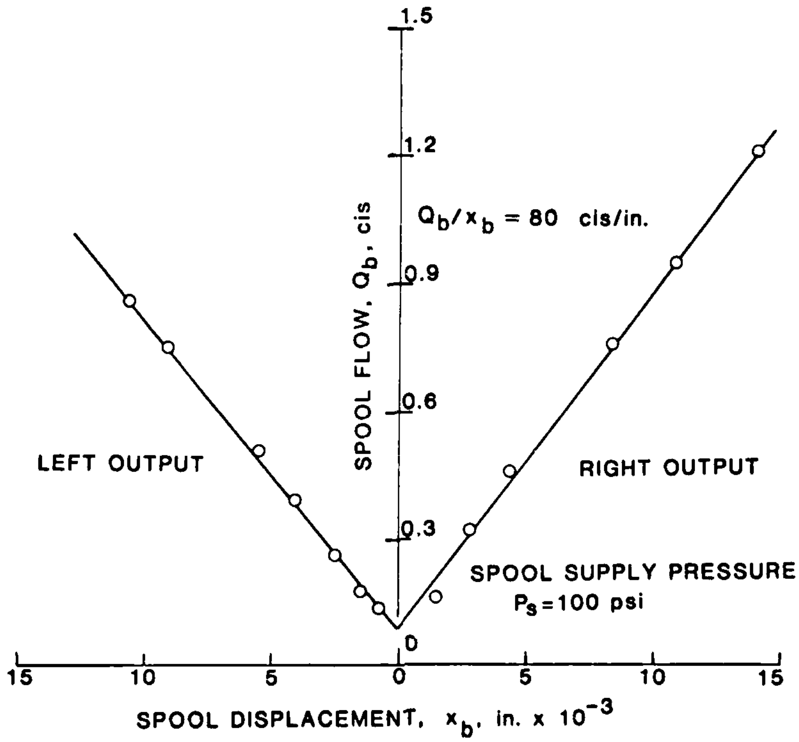

Figure 10. Spool valve flow characteristic.

and spool output pressure pulses can be measured. A variable-speed motor and an eccentric drive were selected to drive the actuator. Use of the eccentric drive not only permits determination of the derivative piston pressures for various frequencies and settings of the derivative resistance, R_b, but allows determination of the phase relationship between x_a and P_b. The theory of operation of the derivative feedback holds that P_b is proportional to $\dot{x}_a$. Since $\dot{x}_a$ is theoretically 90° out of phase with x_a, it follows that P_b should be 90° out of phase also. Yet, intuitively it can be seen that at high values of R_b, as when the derivative resistance valve approaches being completely closed, P_b must of necessity be in phase with x_a. The harmonic oscillation test will establish this phase relationship.

In regard to the proper setting of the derivative resistance R_b, the performance prediction curve of Figure 8 shows that values of A'/A_A of 0.1, or slightly less, should result in an order-of-magnitude increase in bandwidth from that obtained without derivative feedback. To obtain A'/A_A = 0.1, the required setting of the resistance R_b is found from equation (2) and the defined relationship:

$$A' = A_A - K_B \tag{6}$$

from which, for $\frac{A'}{A_A} = 0.1$,

$$K_B = A_A \left(1 - \frac{A'}{A_A}\right) = 0.2\ (1-0.1) \approx 0.180\ \text{in.}^2$$

Using equation (2) and known values for spool area, piston area, spool flow characteristic, and spool spring rate:

$$K_B = 0.180 = \frac{(0.0123)(0.0308)(80)}{50} R_b = 6.06\ (10^{-4}) R_b \tag{7}$$

and $R_b = 297$ psi/cis

For other values of A'/A_A, equation (7) can be used in a more general form:

$$R_b = 1650\ K_B \tag{8}$$

Demonstration of the ability to satisfy equation (8) can be made by a careful calibration of the resistor valve at the pressure differentials expected. An estimate of P_b levels can be made for the case where the derivative piston is driven at 5 Hz at an amplitude of $\pm$0.2 inch. For this condition, the velocity is given by

$v = a_o \omega \cos \omega t$, where $a_o = \pm 0.2$ in.

$$v_{max} = a_o \omega = 0.2\ (2\pi)(5) = 6.28 \text{ in./sec} \tag{9}$$

$$\text{then, } P_b = A_{b1} R_b v_{max} = (0.0123)(297)(6.28) = 23 \text{ psi} \tag{10}$$

Calibration of the resistor valve was accomplished by means of a Whitey Model 22RS4 metering valve (0.020-in. orifice). This valve has a 10-turn micrometer handle that permits repeatable settings to 1/25 of a turn. Resistance measurements were required for flow in both directions, since the valve is designed for flow in one direction only.

A conclusive demonstration of the derivative feedback circuit would, of course, require that it operate in accordance with predictions in a fully assembled servovalve. At the point in time when the component criteria of this section were formulated, it was not possible to have the breadboard reassembled, with the new rotary splitters. Consequently, demonstration criteria were based mainly on the use of the mechanical eccentric drive to allow measurement of P_b and spool flow under simulated servovalve action. However, as the eccentric drive tests progressed, it was felt that the information being obtained was not wholly convincing. As a result, the complete servovalve breadboard was assembled and limited frequency response tests were conducted. The results of these tests are discussed later in this report.

AMPLIFIER PERFORMANCE CRITERIA

The servovalve is designed to accept and sum both fluidic and electrical input control signals. This is accomplished through the use of movable flow splitters. The input amplifier employs a movable splitter actuated by an electrical torque motor. Motion of this splitter, in response to an electrical input signal, results in a proportional output that is used to drive the second amplifier. Fluidic signals are superimposed on the movable splitter with the resulting pressure output being the sum of the outputs that would have occurred if the pressure and electrical signals were applied separately. In the earlier program (Reference 1), the splitter was moved in translation across the amplifier (Figure 4). The movable splitter was parallel sided. It was made by flattening a segment of 0.025-in.-diameter stainless steel wire. This design accomplished the summing objective, but with several limitations:

- Amplifier pressure gain was less than 3.0.
- The summing range was only about ± 3% of the supply pressure.

- Structural rigidity of the splitter was inadequate. Vibration of the splitter caused a noisy signal output, and splitter mechanical failure was frequent.

As a result of these drawbacks, other shapes were evaluated. It was determined that a tapered splitter shape permitted higher pressure gain to be realized. It was also found that by rotating the splitter rather than translating it, a more linear pressure output could be obtained in proportion to the input motion, and that the summing range was extended beyond the original ± 3% of supply pressure.

The pressure criteria for the amplifiers, therefore, are:

- Pressure gain (output blocked) shall exceed 3.0.
- Rotation of the movable splitter shall null (or sum) pressure input signals to at least ± 3% of the supply pressure.
- There shall be no evidence of splitter vibration or structural failure during testing.

The first two criteria, above, can be demonstrated by generating two sets of curves: ΔP_O vs. ΔP_C for several fixed angles of splitter rotation, and ΔP_O vs. splitter angle for several fixed values of ΔP_C. The third criterion can be judged qualitatively by observation of the test records.

Mechanization of the rotary splitter drive by use of a torque motor was not attempted during this program. Early tests showed that the effective range of rotation of the splitter was approximately ± 25°. The torque motor used in the earlier program had an output travel of only ± 0.01 in. Coupling this motor directly to the splitter would have required a drive arm radius of about 0.02 in. length. The mechanical design problem of constructing a reliable mechanism in this dimensional range was considered to be beyond the scope of the present effort. However, in order to generate a harmonic amplifier output signal to test the derivative feedback circuit, a mechanical eccentric drive was coupled to the rotary splitter.

TEST PROCEDURE AND RESULTS

DERIVATIVE FEEDBACK COMPONENTS

To determine the frequency response characteristics of the derivative feedback circuit, it was necessary to provide a harmonic input excitation. With a complete servovalve, this would be accomplished by a sinusoidal input to the first stage amplifier. The actuator, responding to the amplifier output, would oscillate the derivative feedback circuit. To simulate this input to the feedback circuit, an eccentric drive, powered by a variable speed motor, was linked to the actuator piston. The eccentric drive wheel had two radial offset positions allowing actuator drive amplitudes of $\pm$ 0.10 and $\pm$ 0.186 inch. The drive frequency range was from 0.5 to 5.2 Hz. A linear variable differential transformer (LVDT), Shaevitz Model E500, was used to measure actuator stroke. With this setup, the derivative piston was oscillated throughout the 0.5- to 5.2-Hz frequency range, and the resulting time history of pressure (P_b) was recorded for various values of the derivative resistor (R_b). A useful feature of this setup was an auxiliary drive motor shaft that could be turned by hand. This permitted precise positioning of the derivative piston so that static measurements of P_b could be obtained. The test results are given in the following paragraphs.

Derivative Resistance, R_b

The metering valve used for R_b had a micrometer vernier 10-turn handle that permitted precise setting to 1/25 of a turn. Resistance was measured by applying pressures of 5 through 50 psi and measuring the flow of MIL-H-5606 fluid at valve-open settings of 2, 4, 6, 8, and 10 turns. Flow rates were extremely low, so measurements were made using a graduated beaker and stopwatch over intervals ranging from 15 seconds to 5 minutes. Since the metering valve was designed for flow in one direction only, measurements were made in both directions to determine the effects of reversed flow direction. The results are shown in Figure 11. To facilitate using the valve as a resistor, the data of Figure 11 (using the mean values for bidirectional flow) are cross-plotted in Figure 12. These curves show that the valve has a satisfactory range to meet the requirements of $R_b = 297$ psi/cis (Equation 7).

Derivative Piston Assembly

The pressure-stroke characteristics of the derivative piston were determined by closing the resistor valve and slowly moving the piston in and out of the pressure chamber. A typical pressure-stroke curve is shown in Figure 13. This curve shows that the effectiveness of the piston is much less on the negative pressure half of the stroke than on the positive side. This follows from the fact that although pressures in excess of 60 psi could be developed on the compression half of the stroke, the theoretical limit on the negative side is 14.7 psi (atmospheric pressure). To overcome this limitation, an accumulator was used to pressurize the derivative piston chamber, providing an elevated baseline pressure bias. This had the effect of raising the operating pressure range up to the more linear part of the pressure curve, as shown in Figure 14.

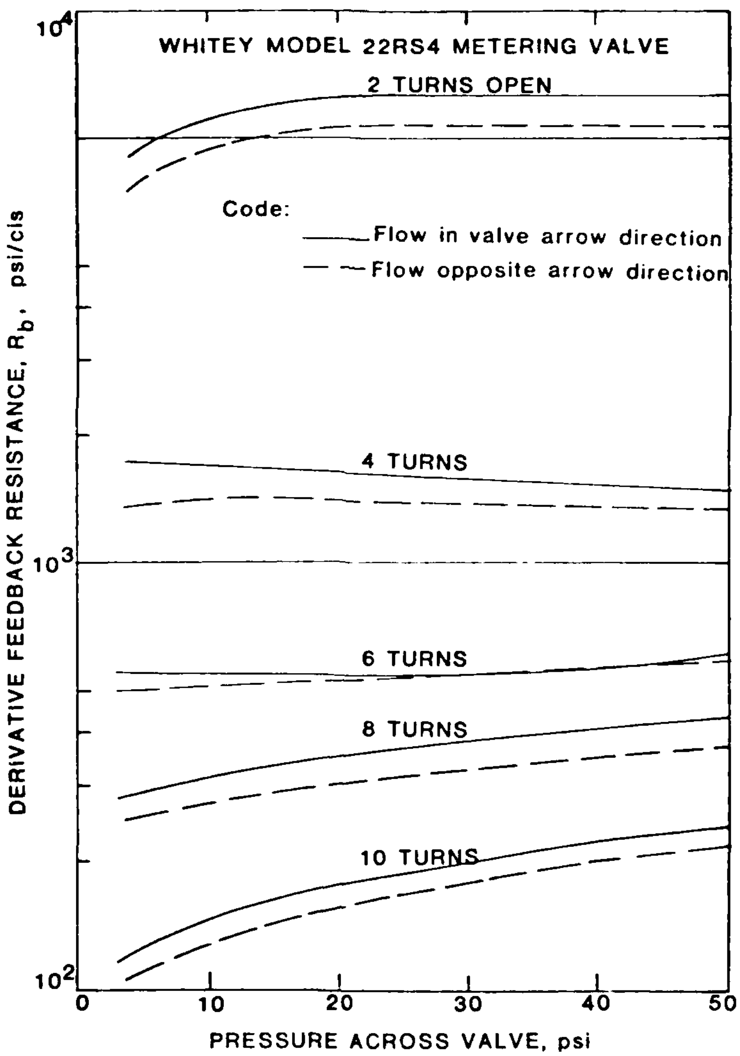

Figure 11. Resistor valve calibration.

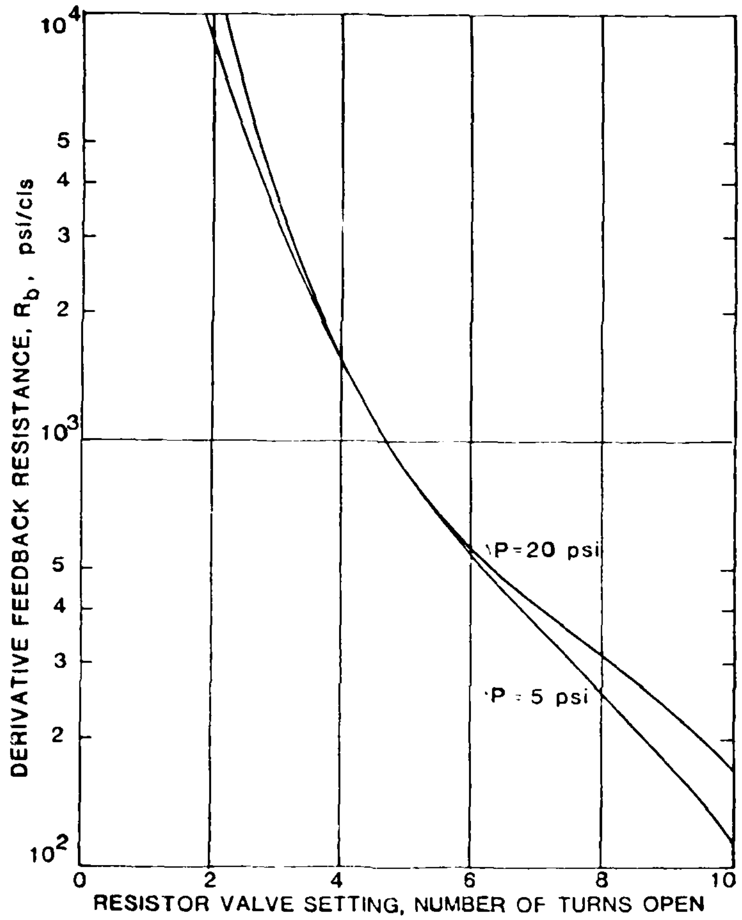

Figure 12. Resistor valve settings.

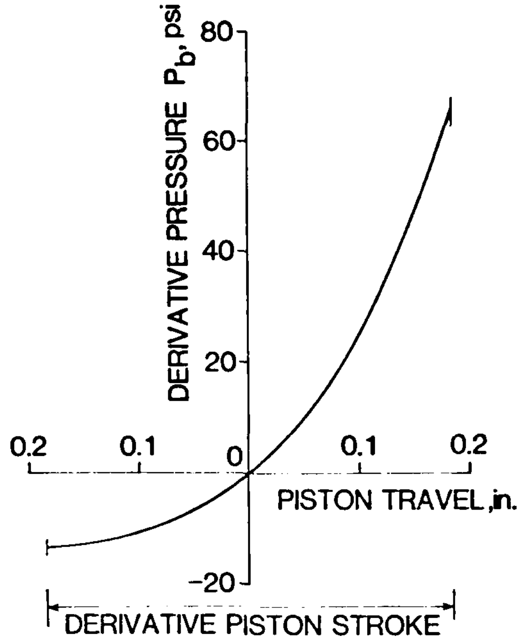

Figure 13. Derivative pressure/stroke, no bias.

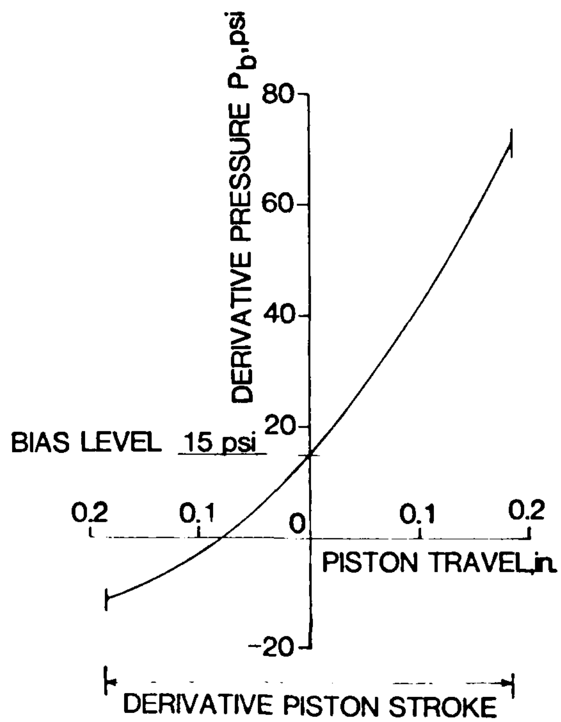

Figure 14. Derivative pressure/stroke, 15 psi bias.

With a bias pressure of 15 psi on the piston chamber, tests were run to verify the assumption that the pressure P_b was a function of actuator velocity $\dot{x}_a$. Using the eccentric drive, the piston was oscillated at amplitudes of $\pm$ 0.1 and $\pm$ 0.186 inch over the available frequency range of 0.5 to 5.2 Hz. Using an LVDT on the actuator piston and a Pace pressure transducer for P_b, x-y recorder plots were obtained of x_a vs. P_b. Since the eccentric drive provided essentially sinusoidal motion, the relationship $\dot{x}_{max} = 2\pi f\ (x_a)$ was used to calculate peak piston velocities. The measured pressures were than plotted against piston velocity (Figure 15). Simultaneously with the x-y plots, the LVDT and pressure signals were fed into a Hewlett-Packard Model 3575A gain-phase meter. Graphs of the phase relationship between P_b and x_a are given in Figure 16. The x-y plots of x_a vs. P_b formed Lissajous figures that illustrate the change in phase between P_b and x_a as the resistance R_b was varied. A typical example is shown in Figure 17, where each Lissajous ellipse was generated by a particular open valve setting of 2, 4, 6, 8, 9, or 10 turns. Phase can be deduced from the proportions of each elliptical figure (Reference 2).

An important assumption made in the derivative feedback theory is that the feedback action is a linear function of actuator velocity (rather than actuator displacement). The curves of Figure 15 show that this assumption is correct for low resistance values, but that as the resistor valve is closed (the upper curves of Figure 15), the pressure response to velocity becomes increasingly nonlinear. In fact, for 4 and 2 turns open (10,000 and 1,600 psi/cis), the curves reverse direction between 2 and 3 in./sec and P_b actually decreases with increasing velocity. A dashed line drawn across the upper portion of Figure 15 indicates the upper boundary of the region in which the resistor valve can be considered to act in reasonable conformity to theory as far as pressure is concerned.

Of equal importance to the pressure-velocity assumption is the requirement that the pressure be generated in the proper phase relationship to the piston velocity. If the pressure pulses are not phased properly, it is evident that the resulting spool action will not provide flow at the proper timing to effectively augment the amplifier flow. In theory, the piston velocity, $\dot{x}_a$, will be 90° ahead of the piston displacement. Figure 16 shows the phase angles for the same valve settings as in Figure 15. It can be seen that with the

---

2 Charles A. Belsterling, FLUIDIC SYSTEMS DESIGN, New York, John Wiley & Sons, 1971, pp. 92-95.

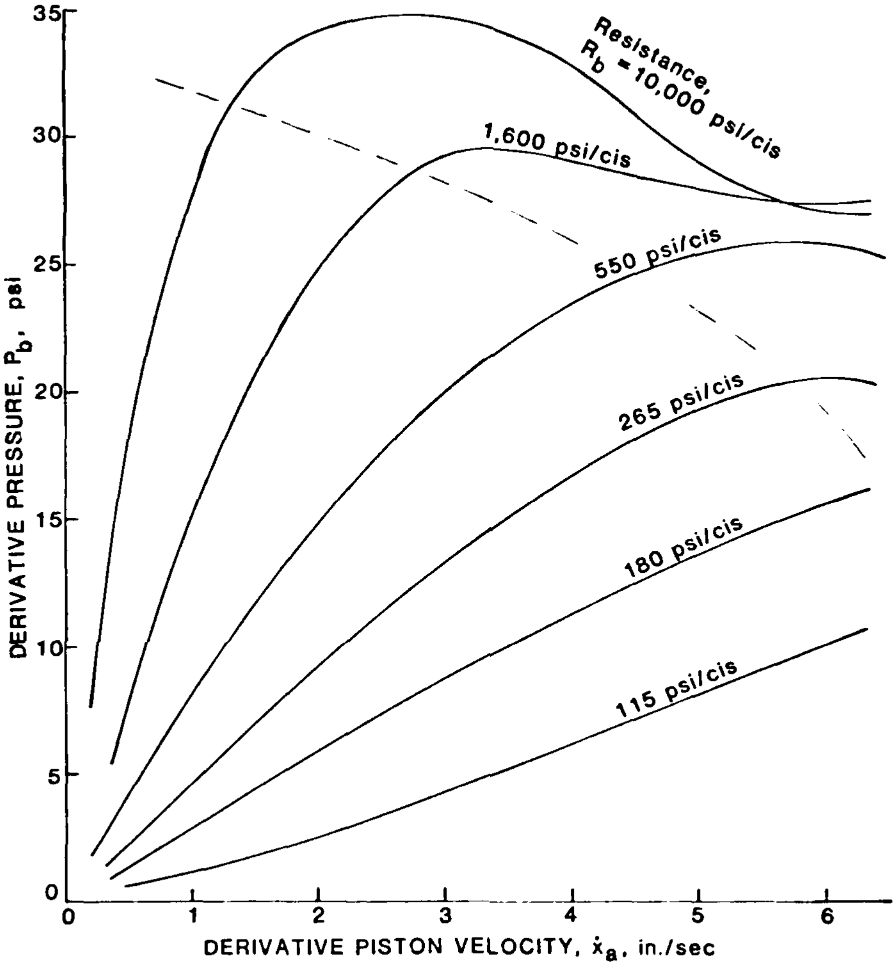

Figure 15. Derivative pressure vs. piston velocity.

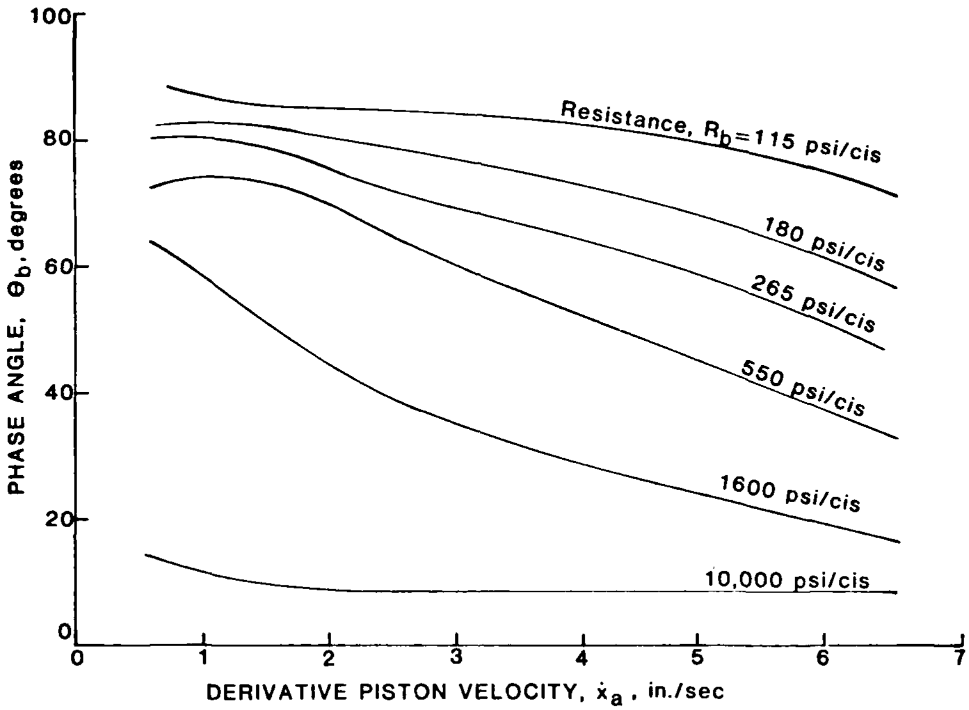

Figure 16. Derivative pressure phase vs. piston velocity.

valve set at 10 turns open ($R_b = 115$ psi/cis), the measured phase is close to 90° at low velocities, and gradually drops to about 80° above 6 in./sec. As the valve is closed (increasing resistance), the phase angle decreases. The upper three curves, representing 10, 9, and 8 valve turns open, are all above 60°, a range in which we might expect reasonably effective feedback action. At higher resistances the action would probably be ineffective.

The intuitive reasoning, expressed in the earlier discussion of derivative feedback theory, that with the resistor valve closed the pressure would be in phase with piston displacement, is confirmed by the lowest curve of Figure 16. This curve is for the valve open only two turns, having a resistance of 10,000 psi/cis. This shows the pressure to be only 10° out of phase with the piston stroke over the whole velocity range.

Figure 17 gives a qualitative picture of the relationship of P_b to the piston stroke. The curves of Figure 17 were created by driving the x-axis of a recorder with the actuator displacement signal and the y-axis with the pressure signal while oscillating the piston at a low frequency (1 Hz). At high resistance (2 turns open), the trace is nearly a straight line slanting from lower left to upper right, indicating that the signals are very nearly in phase. As the valve is opened, the traces become elliptical with the tilted axis becoming more nearly vertical until at 10 turns open the axis is vertical, indicating a 90° phase angle.

It is interesting to note that as the valve is opened, and as the phase becomes more favorable, the pressure decreases from about 40 psi to only about 15 psi. This illustrates one of the problems of sizing the servovalve, namely, that the more closely the assumptions for velocity and phasing are met, the less pressure there is for operating the spool valve. If lighter spool valve springs are used to compensate for the lower pressure, friction effects start to become felt. The present spool valve springs of 50 lb/in. stiffness are the result of many iterations using springs ranging from 5 lb/in. all the way up to the original 600 lb/in. springs that were used in the earlier program for the initial test runs. Each spring rate calls for a different range of derivative resistances to obtain the desired feedback term, K_B.

The conclusion to be drawn from the foregoing discussion is that the derivative piston can be expected to work effectively only for the lower end of the resistance range of the valve used. At more than 550 psi/cis (that is, open less than 6 turns), the pressure response deviates too far from the velocity and phase requirements to expect effective functioning.

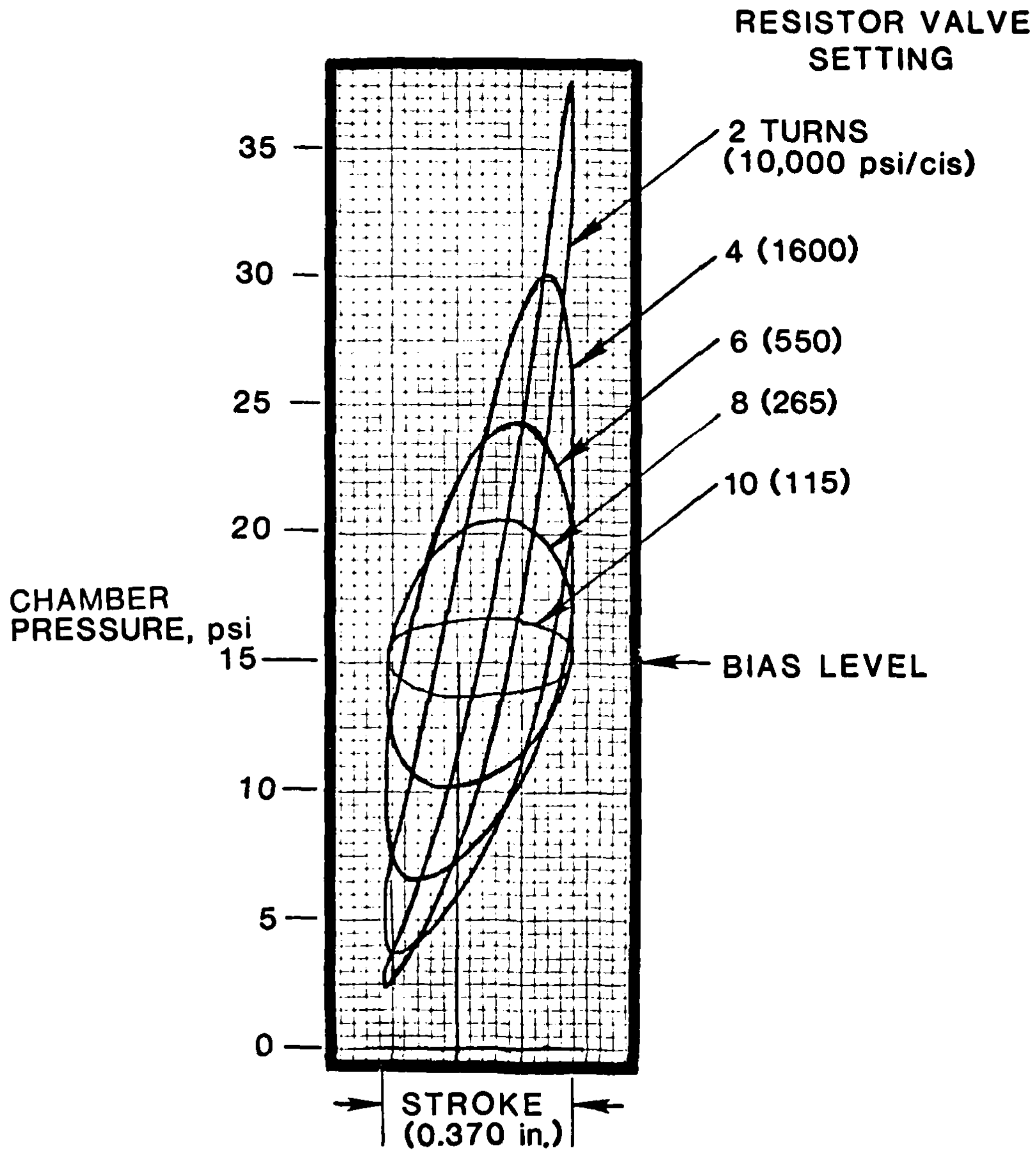

Figure 17. Derivative chamber pressure/ stroke relationship.

Spool Valve

The parameter Q_b/x_b was measured for spool supply pressures of 50, 100, and 200 psi. With the resistor valve closed, the derivative piston was advanced to build up the pressure, P_b, in increments. The resulting spool valve flow was measured and the results plotted in Figure 18.

In Figure 18, the slope of the 100-psi line is

$$Q_b/P_b = \frac{1.3 \text{ cis}}{25 \text{ psi}} = 5.2 \times 10^{-2} \text{ cis/psi.}$$

This compares well with the calculated value of 4.93 x 10^{-2} (see equation (5)).

Since we now have measured values for Q_b/x_b, Q_b/P_b, and A_{b2}, we can put these values in equation (4) and solve for k_b to determine the effective spool spring rate:

$$k_b = \frac{A_{b2}\ (Q_b/x_b)}{Q_b/P_b} = \frac{0.0308(80)}{5.2(10^{-2})} = 47.4 \text{ lb/in.}$$

Actual measurement of the spool springs gave k_b = 49.0 lb/in. This confirms that the effective spring rate is essentially equal to that assumed for the calculations.

Derivative Feedback Circuit

An attempt was made to demonstrate the positive derivative feedback process on a component level, i.e., without the assembled breadboard servovalve. The spool valve outlet ports were loaded with a combination of resistance and capacitance to simulate the actuator swept volume. The actuator itself could not be used because the eccentric drive imposed a fixed amplitude on the piston and the gain effects of the derivative flow could not be measured. Since no instrumentation was available that could be used to measure instantaneous values of the oscillating flow from the spool valve, the spool output pressure time-history was recorded, and attempts made to correlate this information with the servovalve mathematical model. Although it was evident from this data that the feedback circuit was functioning, it was judged that this procedure did not provide a truly convincing demonstration. Since the feedback action is intimately related to the actuator stroke and driving amplifier's output, the decision was made to assemble the breadboard and test the feedback circuit as part of an operating servovalve.

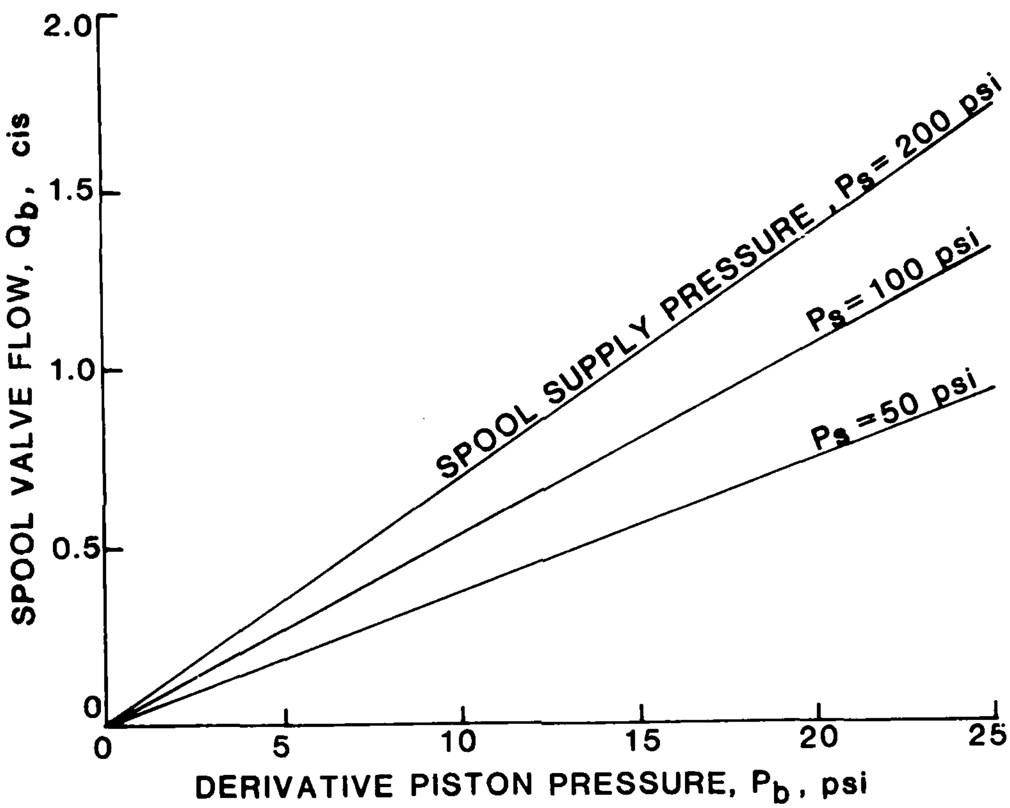

Figure 18. Spool valve flow vs. derivative piston pressure.

The breadboard was assembled in a manner similar to that of the original servovalve (Figure 1). The rotary splitter amplifiers were used, and linkages made to permit oscillation of the first stage splitter through approximately ± 20° using the eccentric drive motor. Actuator position was fed back by another linkage that rotated the second stage splitter through the same angle. Using a first stage supply pressure of 300 psi, second stage supply pressure of 600 psi, and a spool supply of 400 psi (estimated to be 100 psi above the second stage recovery pressure), dynamic response tests were made. A gain-phase meter was used to compare LVDT position signals of the input splitter drive arm and actuator piston. Frequency sweeps were made with no derivative feedback, and with resistor valve settings of 7.5, 7.8, 8.0, 8.6, and 9.0 turns open. These settings represent resistances of 315, 300, 265, 210, and 180 psi/cis respectively. Figure 19 is a Bode plot of the results.

The curves of Figure 19 clearly show a distinct response curve for each of the five resistor valve settings, as well as a curve for no derivative feedback. If the -3 dB level is taken as the bandwidth of each curve, these measured frequencies can be compared with the predicted performance values. Table 1 lists the derivative resistor settings and the corresponding values of bandwidth and A'/A_A.

TABLE 1. MEASURED BANDWIDTH VALUES

RESISTOR VALVE SETTING (TURNS)	RESISTANCE, R_b (psi/cis)	A'/A_A	BANDWIDTH (Hz)
7.5	315	0.045	4.7
7.8	300	0.091	3.7
8.0	265	0.197	2.3
8.6	210	0.364	1.3
9.0	180	0.455	0.5
---	0 (No Feedback)	1.000	0.4

A portion of Figure 8, the predicted system performance curve, is shown in Figure 20 with the measured bandwidth values plotted on it for comparison. It should be noted that during the test, attempts to achieve lower values of A'/A_A were unsuccessful. The resistance values of 315 and 300 psi/cis represent 7.5 and 7.8 turns of the resistor valve. At this point, the servovalve reaction was extremely sensitive to the valve setting. At about 7.5 turns, periods of instability developed and the actuator slammed the stops repeatedly. Even at the 7.8- and 8.0-turn settings, the actuator waveform was somewhat irregular, and the functioning could not be considered completely satisfactory in spite of the good bandwidth agreement with predicted values.

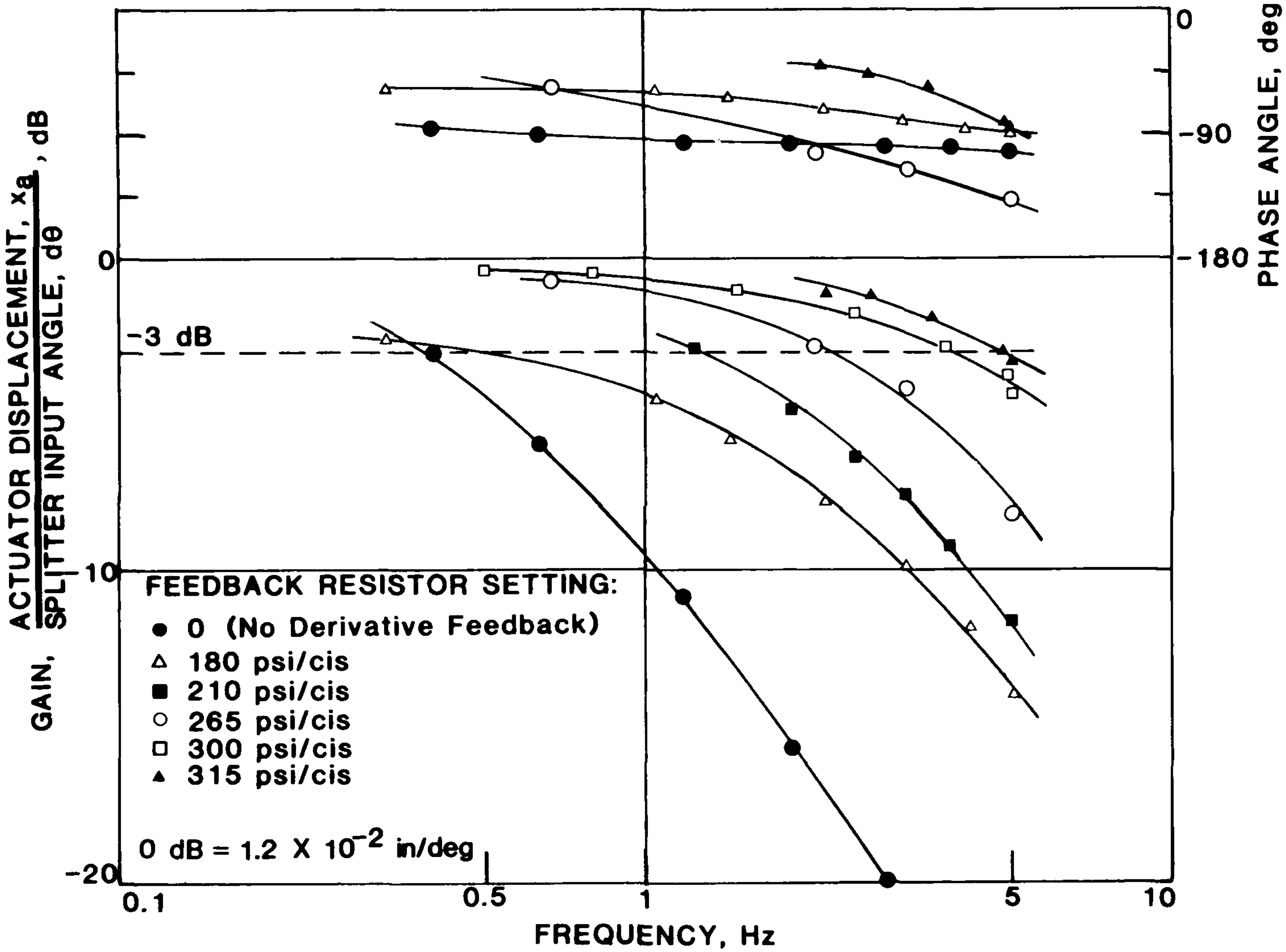

Figure 19. Servovalve frequency response.

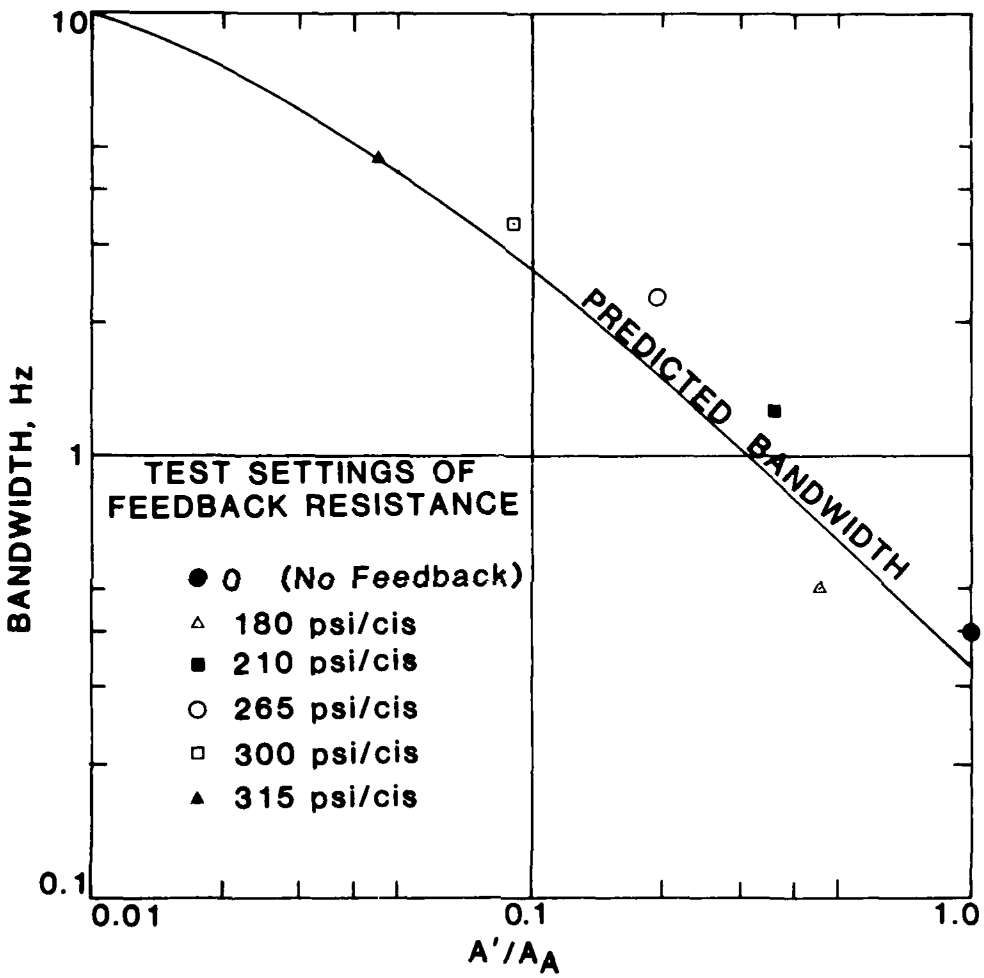

Figure 20. Predicted vs. measured bandwidth.

AMPLIFIERS

Blocked output pressure gain tests were conducted on two rotary splitter amplifiers. Both amplifiers had identical rotary splitters, but each incorporated a different means of supporting and rotating the splitters. In one design, the splitter was inserted from above, through the amplifier laminate, into a 1/4-inch-diameter turntable in the amplifier base. In the other design, the splitter, machined integrally with a 0.07-inch-diameter drive rod, was inserted through the amplifier base into the amplifier cavity. Functionally, both arrangements were designed to have the same performance. The advantage of the second design was that it permitted removal and insertion of the splitter without disassembly of the amplifier stack; also, it was a simpler and more economical design. The gain tests showed that the second design had an average pressure gain of only 2.6 as compared with gains in excess of 4.0 for the first design. Examination of the amplifiers showed that due to machining difficulties, the splitter rotational axis in the lower gain amplifier was located approximately 0.003 in. too far upstream, resulting in a void between the moving and fixed splitter parts. Further study is required to determine the best rotating splitter position to optimize gain.

Typical gain test results from the higher gain amplifier are shown in Figure 21. This figure shows that a family of pressure gain curves exists, one for each fixed angular orientation of the rotary splitter. The parallelism and uniform spacing of the curves is an indication of the summing ability of the amplifier. At a splitter angle of $\pm$ 25°, the rotary splitter was able to null control pressures of $\pm$ 5% of the supply pressure, exceeding the $\pm$ 3% ability of the translating splitter.

A similar family of curves is obtained if the splitter is rotated at fixed increments of ΔP_C control pressure. For clarity, one such curve is shown in Figure 22 for rotation of the splitter with $\Delta P_C = 0$ psi.

During the testing there was no evidence of splitter vibration of structural fatigue failure.

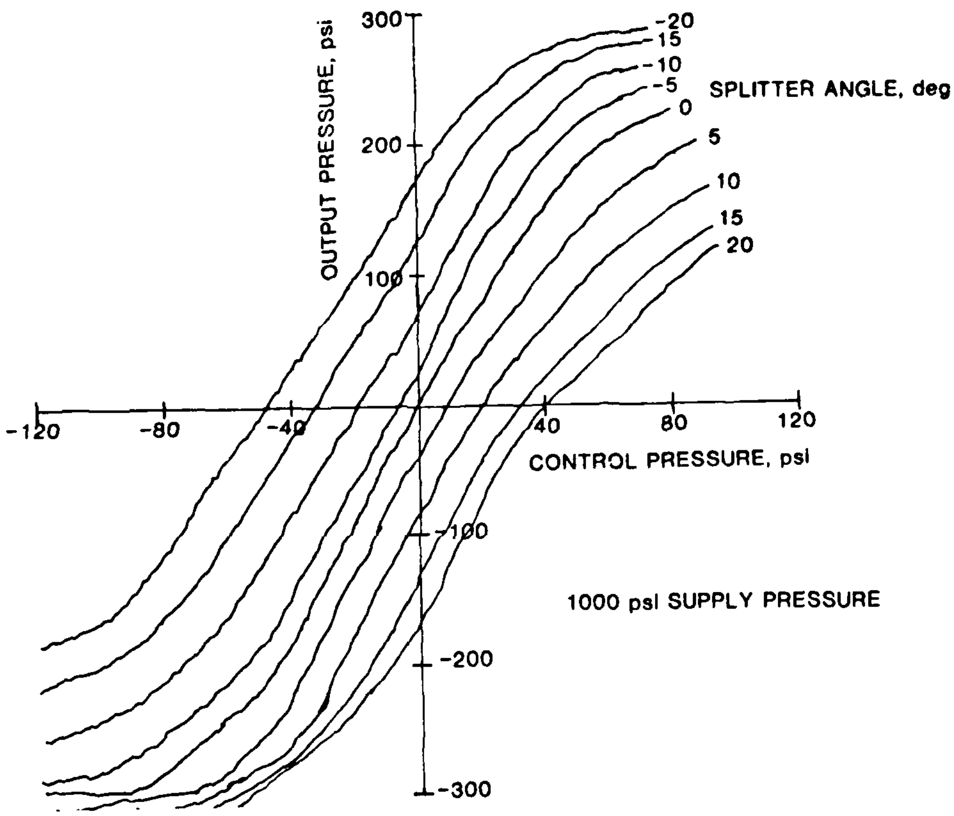

Figure 21. Pressure gain for various splitter angles.

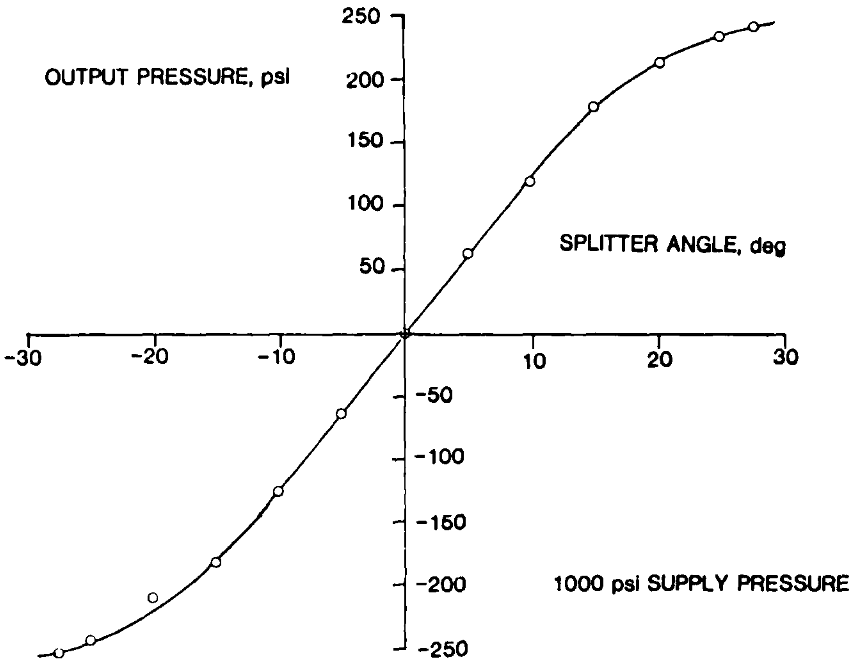

Figure 22. Amplifier output pressure vs. splitter angle.

CONCLUSIONS

Both the rotary splitter amplifier and positive derivative feedback concepts were satisfactorily demonstrated. Specific program achievements were:

- Ability to accept and sum fluidic and mechanical inputs confirmed.
- Reduced rotary splitter friction compared to translating splitter.
- Improved amplifier pressure gain (4 to 5 compared to 2 to 3 of earlier program).
- Linear amplifier pressure output proportional to rotary splitter angular position.
- Freedom from splitter vibration and structural fatigue failure.
- Mathematical model validity confirmed.
- Order-of-magnitude increase in bandwidth achieved by use of positive derivative feedback.

Although the positive derivative feedback circuit functioned well, there was occasional loss of actuator position control in this mode of operation. This appeared to be caused by an inability of the spool centering springs to accurately maintain the spool null position, particularly at higher frequencies. Stiffer spool springs would alleviate this problem, but higher derivative piston pressures would be required to match the higher spring forces.

Servovalve response to electrical inputs was not demonstrated in this phase of the program. This would require a separate design effort to match the rotary splitter to some form of electrical motor. Use of a torque motor (as in the earlier program) presents mechanical difficulties, since torque motor displacement output angles are typically less than $\pm$ 1.0°, while rotary splitter displacement angles are $\pm$ 20 to 25°.

Further refinement of the rotary splitter concept, particularly in fabrication techniques to permit more uniform surface finish and contour, will result in uniformly high amplifier gain. As a result of this program, sufficient data and experience are now available to allow design and fabrication of a high performance pre-production prototype servovalve.

RECOMMENDATIONS

In order to maximize the benefits made possible by the servovalve development program to date, the following steps are recommended:

- Evaluate alternates to a torque motor for coupling rotary splitter to electrical input.
- Improve spool valve null position characteristics.
- Design, assemble, and test an improved breadboard servovalve (pre-production prototype).

LIST OF SYMBOLS

A_A	actuator piston area, in.^{2}
A_{b1}	derivative piston area, in.^{2}
A_{b2}	spool area, in.^{2}
A'	$A_A - K_B$, in.^{2}
a_o	maximum piston displacement, in.
B	load viscous damping, lb sec/in.
C_a	actuator compliance, in.^{3}/psi
G	amplifier gain
i	current, amperes
K_y	jet displacement per pressure difference, in./psi
k_b	spool spring rate, lb/in.
K_B	derivative feedback coefficient, in.^{2}
K	load spring rate, lb/in.
M	load mass, lb sec^2/in.
P_+	amplifier supply pressure, psi
P_s	spool supply pressure, psi
P_b	derivative piston pressure, psi
P_o	amplifier output pressure, psi
P_c	amplifier input pressure, psi
Q_b	spool flow rate, in.^{3}/sec (cis)
R_o	amplifier output resistance, lb sec/in.^{5}
R_ℓ	actuator leakage resistance, lb sec/in.^{5}
R_b	derivative resistance to ground, lb sec/in.^{5}
R'	$R_\ell/(R_\ell + R_o)$
r_x	actuator position feedback ratio

LIST OF SYMBOLS (Cont'd)

s	Laplace operator, sec^{-1}
v	piston velocity, in./sec
x_a	actuator displacement, in.
x_b	spool displacement, in.
x_j	mechanical input, in.
x_s	spool position, in.
y/i	torque motor displacement coefficient, in./ampere
Z_ℓ	load impedance, lb/in.
ζ	damping ratio
ω	circular frequency, rad/sec
θ_b	derivative pressure phase angle, deg